Experimental characterisation of a metamaterial optical partial polariser in the quantum regime

S. A. Uriri, T. Tashima and M. S. Tame

School of Chemistry and Physics, University of KwaZulu-Natal, 4000, Durban, South Africa

E-mail: `markstame@gmail.com`

Abstract. Metamaterials have opened up many novel ways of controlling light, and in particular, controlling the polarisation of light. An important component in this respect is the polariser, which transmits light of one polarisation while blocking light of another polarisation. In our work, we experimentally probe and characterise a metamaterial polariser in the quantum regime. To do this, we prepare different polarisation-encoded single-photon states and send them through the metamaterial. We then perform quantum state tomography and obtain output states with a high fidelity to those expected ($\gtrsim 96\%$ on average). The transmission of vertically polarised light increases from 75% to 85% as the nanorod dimensions vary in the metamaterial. On the other hand, the metamaterials consistently transmit 99% of horizontally polarised light. The results are in full agreement with our theoretical predictions for an optical polarizer, in which we employ an analytical model for the metamaterial. Our study provides further evidence that metamaterials may be used for building compact optical components in on-chip quantum photonic systems.

1. Introduction

Plasmonic metamaterials are made from metallic nanostructures engineered with feature sizes smaller than the wavelength of interest [1]. They are able to achieve unusual optical responses that are not available in nature [2]. The metallic nanostructures in metamaterials, also known as 'unit cells', are usually arranged periodically in close range to each other, and their material and geometrical properties can be manipulated in order to change the bulk permittivity ϵ, permeability μ and other properties of the material. The unusual optical behaviour of metamaterials is due to the collective oscillations of the nanostructures in resonance with the incident light, *i.e.* a localised surface plasmon resonance [3, 4]. This plasmonic resonance gives metamaterials the ability to control and manipulate many different aspects of light.

Controlling the polarisation of light is an important process in many areas of science and technology, for example in communication [5], imaging [6, 7], and sensing [8]. Over the years, conventional optical polarisers have been made from birefringent materials [9], and from crystals or polymers [10]. Recently, the control of the polarisation of light using metamaterials has become possible. Shen *et al.* [11] have demonstrated an ultra-high efficiency metamaterial polariser, where light that is perpendicular to the principal axis is transmitted undisturbed, while light that is parallel is attenuated. Tam and Yan [12] have designed a plasmonic ultra-broadband polariser based on silver nanowire arrays where a broadband transmission was realised. Chin *et al.* [13] have shown that, with designed metamaterials mimicking anisotropic crystals, it is also possible to change the polarisation state of the field during the polariser operation.

In our work we experimentally probe and characterise a plasmonic metamaterial polariser in the quantum regime. We prepare different polarisation-encoded single-photon states and send them through the metamaterial. We then measure the output states of the metamaterial by performing quantum state tomography. An optical polariser that can control and manipulate the polarisation of light is an important component in quantum computing and quantum communication, where quantum information is encoded into the polarisation degree of freedom of single photons [14]. Due to the small size of the metamaterial it can be integrated with other optical components at the nanoscale in the design of an on-chip optical system. Along these lines, recently Asano *et al.* [15] used an optical metamaterial polariser to perform quantum state engineering, realising a quantum entanglement distillation protocol. Here, we extend this study by comparing the predictions of the expected theoretical response of the metamaterial using an analytical model to the experimental results obtained in the quantum regime.

2. Experimental setup

The experimental setup is shown in figure 1 (a), where type-1 spontaneous parametric down-conversion is used to generate pairs of single photons [16, 17]. A pump laser at 405 nm is rotated to vertical polarisation by a half-wave plate (HWP). The pump beam is then sent through a non-linear BiBO crystal, which produces two 'twin' (idler and signal) photons polarised horizontally at a lower frequency (wavelength 810 nm). One photon is produced in arm A and the other in arm B. The optical axis of the BiBO is cut such that the two photons emerge at 3^0 from the initial pump direction. A single photon in arm A is used to herald the presence of another single photon in arm B. A qubit is encoded into the single photon in arm B using a quarter-wave plate (QWP) and HWP. Here, the polarisation states $|H\rangle$ and $|V\rangle$ are used as the orthogonal basis states of the qubit. This qubit is then sent through the plasmonic metamaterial (MTM).

Quantum state tomography is performed on the output of six different polarisation-encoded qubits sent through the metamaterial using a QWP, HWP and a polarising beamsplitter (PBS). This allows the density matrices to be reconstructed via projective measurements [18]. The output of our projective measurement is sent into fibre couplers and coincidence counts between
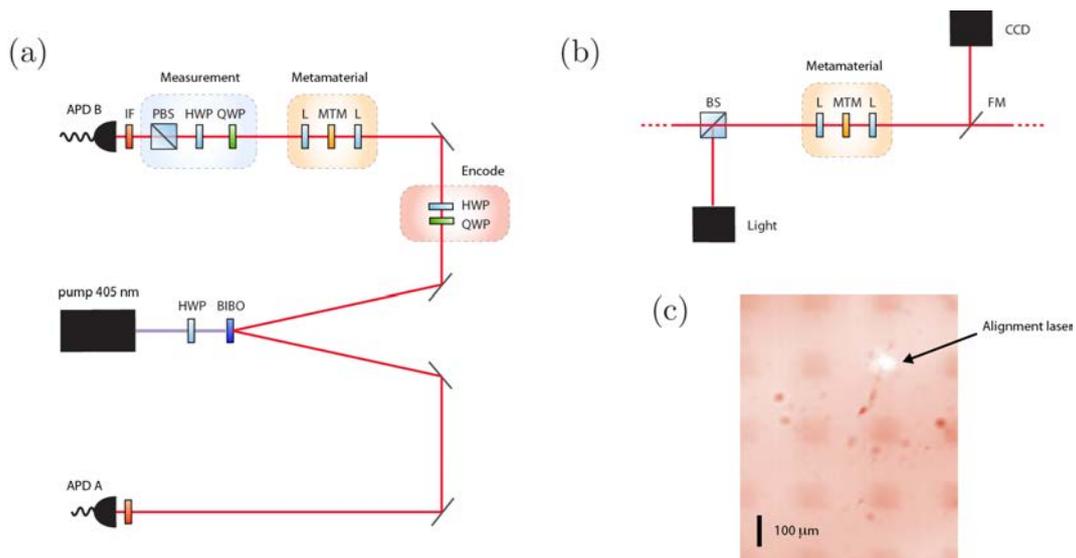
Figure 1: Overview of the experiment. (a) Experimental setup. Here, L is a convex lens, HWP and QWP are a half- and quarter-wave plate, BiBO is a nonlinear crystal, MTM is a metamaterial, PBS is a polarising beamsplitter and APD is an avalanche photodetector. (b) Telescope system for imaging the alignment laser and its position on different metamaterials. FM is a flip mirror. (c) Image of metamaterials with the alignment beam on a particular design.

arm A and B (8 ns window) are detected by silicon avalanche photodetectors and a coincidence counting unit. An interference filter (800 ± 20 nm) is placed in front of each fibre coupler to cut out photons of higher and lower frequencies corresponding to unwanted down-conversion processes and the pump beam. Figure 1 (b) shows the telescope system used to focus the single photons onto the metamaterial and CCD for imaging. Figure 1 (c) shows an image obtained from the CCD displaying the sample used with different metamaterial designs (each $100\mu m \times 100\mu m$). An alignment beam (785 nm) sent from the fibre coupler can be seen at one of the metamaterial designs. The telescope system is designed in such a way that the beam before and after the lenses is collimated and therefore the beam diameter of single photons traversing in the opposite direction will be roughly the same as that of the alignment beam. When single photons are used in the setup the beamsplitter and mirror in figure 1 (b) are flipped down.

3. Quantum state probing

The input probe states are encoded experimentally by using a QWP and HWP set at a particular angle (see encode box in figure 1 (a)). The unitary operations of the wave plates acting on the polarisation qubit of the single photon in arm B are given by

$$\hat{U}_{QWP}(q) = \frac{1}{\sqrt{2}} \begin{bmatrix} i - \cos(2q) & \sin(2q) \\ \sin(2q) & i + \cos(2q) \end{bmatrix}, \qquad \hat{U}_{HWP}(h) = \begin{bmatrix} \cos(2h) & -\sin(2h) \\ -\sin(2h) & -\cos(2h) \end{bmatrix}. \quad (1)$$

By choosing the angles correctly [18] we obtain six different polarisation-encoded qubits

$$|H\rangle = \begin{pmatrix} 1 \\ 0 \end{pmatrix}, |V\rangle = \begin{pmatrix} 0 \\ 1 \end{pmatrix}, |+\rangle = \frac{1}{\sqrt{2}} \begin{pmatrix} 1 \\ 1 \end{pmatrix},$$

$$|-\rangle = \frac{1}{\sqrt{2}} \begin{pmatrix} 1 \\ -1 \end{pmatrix}, |L\rangle = \frac{1}{\sqrt{2}} \begin{pmatrix} 1 \\ i \end{pmatrix}, |R\rangle = \frac{1}{\sqrt{2}} \begin{pmatrix} 1 \\ -i \end{pmatrix}, \quad (2)$$

where $|H\rangle$, $|V\rangle$, $|+\rangle$, $|-\rangle$, $|L\rangle$ and $|R\rangle$ correspond to horizontal, vertical, diagonal, anti-diagonal, left- and right-circularly polarised single photons, respectively. We send these probe states through the metamaterial and perform quantum state tomography on the output states.

4. Theoretical prediction

Before discussing the results of probing the metamaterial in the quantum regime we describe the theory of transmission of light through them. For this we model the metamaterial as a periodic array of nanoparticles in a rectangular lattice with periods d_x and d_y. In the dipole approximation, each nanoparticle representing a unit cell of the metamaterial is modelled by a dipole with polarisability tensor $\boldsymbol{\alpha}$, which relates the dipole moment to the local electric field at the particle [19–21]. The plasmonic nanoparticles in this work are rod-like in shape and are well described as an ellipsoid with semi-axes a, b and c. This gives a diagonal polarisability tensor with non-zero elements [20]

$$\alpha_{ii} = 4\pi\epsilon_0 abc \frac{\epsilon_{au} - \epsilon_m}{3\epsilon_m + 3L_i(\epsilon_{au} - \epsilon_m)}, \quad (3)$$

where ϵ_0 is the free space permittivity, L_i ($i = x, y, z$) is a shape factor [20], $\epsilon_{au} = -22.842 + 1.8388i$ is the relative permittivity of gold and $\epsilon_m = (1.45)^2$ the relative permittivity of the surrounding medium (silica) at 810 nm. In our simulation, $a = \frac{l}{2}$, $b = \frac{w}{2}$, and $c = \frac{z}{2}$, where l is the length of the nanorod, w is the width and z is the height. The nanorods are fabricated by electron-beam lithography and gold deposition on a silica substrate [15]. The dimensions used are $d_x = d_y = 200$ nm for the period, $l = 95 - 110$ nm for the length, $w = 39 - 47$ nm for the width and $z = 30$ nm for the thickness. Each metamaterial in figure 1 (c) has a
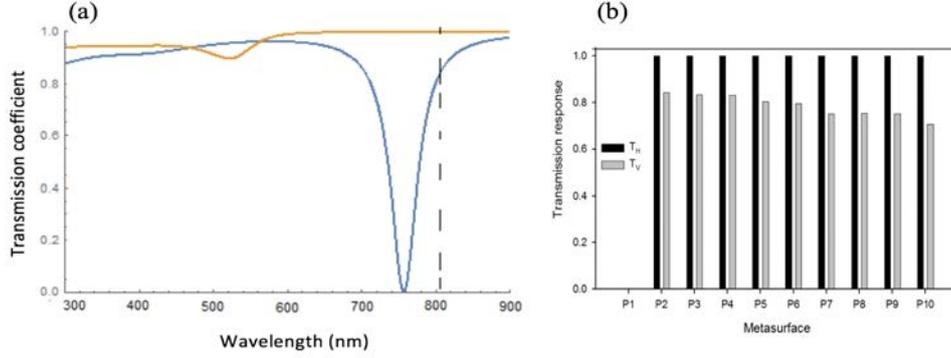
Figure 2: Theoretical and experimental transmission through metamaterials. (a) Theoretical transmission spectra for horizontally (orange line) and vertically (blue line) polarised light sent through a plasmonic metamaterial made of gold nanorods ($w = 39$ nm, $l = 110$ nm, $z = 30$ nm). The dashed line corresponds to 810 nm. (b) Transmission coefficients of horizontally (black) and vertically (grey) polarised single photons (at 810 nm) through different plasmonic metamaterials ($w = 39 - 47$ nm, $l = 110$ nm, $z = 30$ nm) obtained via experiment. Here, metamaterial design 'P10' has the dimensions used in (a) and design 'P1' is an empty slot on the sample.

different dimension chosen for the length and width of the nanorods used as unit cells, with a total square footprint of 100μm$\times100\mu$m. The transmission and reflection of light through this kind of nanoparticle periodic array are described in detail in Ref. [21] and given for light with normal incidence to the array and polarised in direction k as

$$R_k = \frac{i\mu_0\pi fc}{d_xd_y}\alpha_{kk}, \qquad T_k = 1 + R_k. \qquad (4)$$

Here, μ_0 is the free space permeability, f is the frequency of the propagating electromagnetic wave and c is the speed of light in a vacuum. With these equations at hand, we are able to model the transmission of single photons of horizontal and vertical polarisation through the different metamaterial designs shown in figure 1 (c), where the vertical axis of the single photons is oriented along the long axis of the nanorods. From the above theory, this means that the probability of transmitting a photon encoded in the state $|V\rangle$ through a metamaterial should decrease as the nanorod length in the metamaterial increases and width decreases. This is caused by a stronger plasmonic resonance of the nanorod. On the other hand, the transmission of a photon encoded in the state $|H\rangle$ is constant for all the metamaterial designs as the plasmonic resonance is weak along the width of the nanorod for the widths considered.

5. Experimental results

We now present our experimental results and compare them with results obtained via the theory outlined in the previous section. Figure 2 (a) shows the transmission for horizontally and vertically polarised light obtained from theory for a particular set of nanorod dimensions ($w = 39$ nm, $l = 110$ nm, $z = 30$ nm). A dashed line represents 810 nm, corresponding to the wavelength of our single photons. In figure 2 (b) we show the results from experimental probing of several metamaterials in our setup with different nanorod dimensions. The transmission response for $|H\rangle$ and $|V\rangle$ polarisation encoded photons were calculated using $T_H = \frac{T_{H_M}}{T_{H_S}}$ and $T_V = \frac{T_{V_M}}{T_{V_S}}$, respectively. Here, T_{H_S} and T_{H_M} are the transmission probabilities of the state $|H\rangle$ through the substrate (no metamaterial) and through the metamaterial, respectively. Similarly, T_{V_S} and T_{V_M} are the transmission probabilities of the state $|V\rangle$ through the substrate and metamaterial, respectively. As can be seen in figure 2 (b) that the transmission of the state $|V\rangle$ decreases from 85% to 75% as the nanorod dimensions vary in the metamaterial (length and thickness
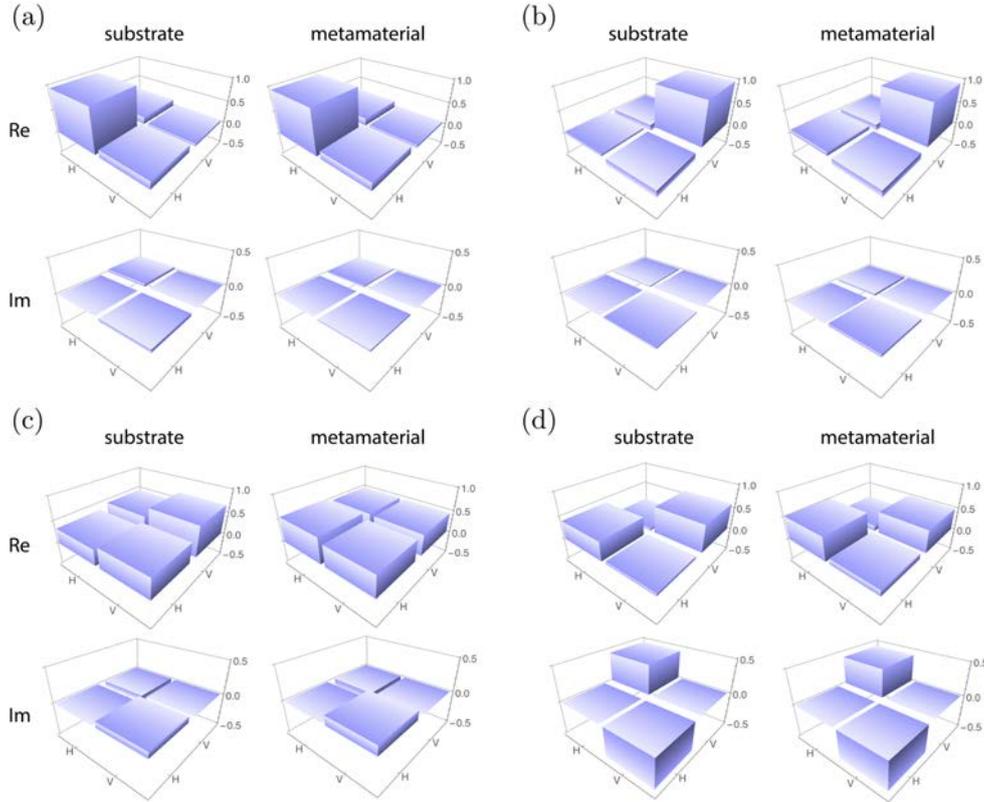
Figure 3: Quantum state tomography of probe states sent through the metamaterial and substrate. (a) Real and imaginary parts of the output state $\hat{\rho}_{exp}$ obtained from the state $|H\rangle$ sent through the substrate and metamaterial. (b) Real and imaginary parts of the output state for $|V\rangle$ sent through the substrate and metamaterial. The other panels show the output states for the following probe states: (c) shows $|+\rangle$ and (d) shows $|L\rangle$.

fixed, width decreases). On the other hand, the plasmonic metamaterials transmit $\sim 99\%$ of the state $|H\rangle$ compared to the bare substrate. In the experimental results in figure 2 (b), the metamaterial design 'P10' has nanorods with the same dimensions as those used in the theory for figure 2 (a). Considering the finite bandwidth of the single photons, the experimental results are in good agreement with the average transmission obtained from the theory. Also, the trend of our results generally agrees with the transmissions obtained by Asano et al. in Ref. [15], which reported transmissions from 11% to 41% for TV by classical FTIR for metamaterials with similar nanorod structures, but a different range of dimensions and thus transmission response.

In order to further investigate metamaterial P10 in the quantum regime we probe it with six polarisation-encoded single photon states: $|H\rangle$, $|V\rangle$, $|+\rangle$, $|-\rangle$, $|L\rangle$ and $|R\rangle$. The fidelity $F = \langle\psi|\,\hat{\rho}_{exp}\,|\psi\rangle$ and purity $P = tr(\hat{\rho}_{exp}^2)$ [22] were then calculated for the output states $\hat{\rho}_{exp}$ obtained using quantum state tomography [18]. Here, $|\psi\rangle$ is the ideal input quantum state and the fidelity provides a measure of the closeness of the output state to the ideal input state. The purity provides a measure of how close the output state is to a pure state. In figure 3 we show the real and imaginary parts of the density matrices for four different probe states ($|H\rangle$, $|V\rangle$, $|+\rangle$ and $|L\rangle$) sent through either the substrate or metamaterial P10. We obtained a fidelity of 0.960 ± 0.002 and a purity of 0.950 ± 0.007 for the probe state $|H\rangle$ transmitted through the substrate, and a fidelity of 0.97 ± 0.003 and a purity of 0.956 ± 0.007 for the state $|H\rangle$ transmitted through the metamaterial. The fidelity and purity of all six probe states are given in table 1.

One can see in figure 3 (a) and (b) that the $|H\rangle$ and $|V\rangle$ states are transmitted through the metamaterial in the same way as the substrate, although with fewer photons detected for $|V\rangle$

State	Fidelity		Purity	
	Substrate	Metamaterial	Substrate	Metamaterial
$|H\rangle$	0.960 ± 0.002	0.970 ± 0.003	0.950 ± 0.007	0.956 ± 0.003
$|V\rangle$	0.960 ± 0.002	0.928 ± 0.003	0.954 ± 0.004	0.925 ± 0.007
$|+\rangle$	0.940 ± 0.003	0.960 ± 0.002	0.946 ± 0.006	0.968 ± 0.005
$|-\rangle$	0.950 ± 0.003	0.910 ± 0.003	0.953 ± 0.006	0.987 ± 0.007
$|R\rangle$	0.924 ± 0.003	0.925 ± 0.003	0.912 ± 0.006	0.954 ± 0.006
$|L\rangle$	0.938 ± 0.003	0.929 ± 0.003	0.938 ± 0.002	0.934 ± 0.005

Table 1: Fidelity and purity for the single-photon probe states.

through the metamaterial. On the other hand, for the $|+\rangle$ and $|L\rangle$ states shown in figure 3 (c) and (d) the metamaterial acts as a partial polariser, balancing the ratio of the diagonal terms.

6. Summary
We experimentally characterised a plasmonic metamaterial optical polariser in the quantum regime and showed that the metamaterial behaves like a partial polariser, transmitting the horizontally polarised component of single photons undisturbed and part of the vertically polarised component. The experimental results are in agreement with the theory. The other metamaterials studied showed polarisation dependence for vertically polarised photons according to the dimensions of the nanorods used as unit cells. The transmission of horizontally polarised photons was essentially constant for all metamaterials. This study provides further evidence that metamaterials may be used as optical components in quantum photonic systems.

Acknowledgments

References
[1] Cai W and Shalaev V 2010 *Optical Metamaterials: Fundamentals and applications* (Dordrecht: Springer)
[2] Barnes W L 2011 *Philos. Trans. R. Soc. London, Ser. A* **369** 3431-3433.
[3] Huttler E and Fendler J H 2004 *Adv. Matter.* **16** 1685-1706
[4] Tame M S, McEnery K R, Ozdemir S K, Lee J, Maier S A and Kim M S 2013 *Nature Phys.* **9** 329-340
[5] Damask J N 2004 *Polarization optics in Telecommunications* (Dordrecht: Springer)
[6] Fang N and Zhang X 2003 *Appl. Phys. Lett.* **82** 161
[7] Fang N, Lee H, Sun C and Zhang X 2005 *Science* **308** 534-537
[8] Chen T, Li S and Sun H 2012 *Sensors* **12** 2742-2765
[9] Tyan R C et al. 1997 *J. Opt. Soc. Am. A* **14** 1627-1636
[10] Land E H 1951 *J. Opt. Soc. Am.* **41** 957-963
[11] Shen B, Wang P, Polson R and Menon R 2014 *Optica* **5** 356-960
[12] Han C and Tam W Y 2015 *Appl. Phys. Lett.* **106** 081102
[13] Chin J Y, Lu M and Cui T J 2008 *Appl. Phys. Lett.* **93** 251903
[14] O'Brien J, Furusawa A and Vuckovic J 2005 *Nature Photon.* **3** 687-695
[15] Asano M et al. 2015 *Sci. Rep.* **5** 18313
[16] Hong C K and Mandel L 1986 *Phys. Rev. Lett.* **56**, 58-60
[17] Burnham D C and Weinberg D L 1970 *Phys. Rev. Lett.* **25**, 84-87
[18] James D F V, Kwiat P G, Munro W J, and White A G 2001 *Phys. Rev. A.* **64** 052312
[19] Zhao Y and Alu A 2013 *Nano Lett.* **13** 1086 - 1091
[20] Bohren C F and Huffman D R 1998 *Absorption and Scattering of light by small particles* (New York: John Wiley & Sons)
[21] Alu A and Engheta N 2011 *Structured Surfaces as Optical Metamaterials* (New York: Cambridge University Press)
[22] Nielsen M A and Chuang I L 2000 *Quantum Computation and Quantum Information* (Cambridge: Cambridge University Press)